Proceedings of the International Symposium of Mechanism and Machine Theory, 2010
AzCIFToMM – Izmir Institute of Technology
5-8 October 2010, Izmir, TURKEY

Integration of the Hybrid-Structure Haptic Interface: HIPHAD v1.0

Tunç Bilgincan, Erkin Gezgin, Mehmet İsmet Can Dede

İzmir Institute of Technology, Department of Mechanical Engineering, Robotics Laboratory
Gülbahçe, Urla, İzmir, Turkey 35430
candede@iyte.edu.tr

Abstract
Design, manufacturing, integration and initial test results of the 6-DoF haptic interface, HIPHAD v1.0, are presented in this paper. The hybrid haptic robot mechanism is composed of a 3-DoF parallel platform manipulator, R-Cube, for translational motions and a 3-DoF serial wrist mechanism for monitoring the rotational motions of the handle. The device is capable of displaying point-type of contact since only the R-Cube mechanism is actuated. The dimensions and the orientation of the R-Cube mechanism are reconfigured to comply with the requirements of the haptic system design criteria. The system has several advantages such as relatively trivial kinematical analysis, compactness and high stiffness. The integration of the system along with its mechanism, data acquisition card (DAQ), motor drivers, motors, position sensors, and computer control interface are outlined.

Keywords: Haptic interface, Parallel manipulators, R-Cube

1. Introduction

Among all senses, touch sense is the most amazing and necessary one. In embryos, it develops and activates before all other senses. It provides information about texture, shape, temperature, weight, etc. of an object or environment. Touch sense is the most durable sense organ because it employs many connections to nervous system from every single part of the body. This complexity also provides reliable sensory inputs to cerebral cortex of the brain. Basically, the mechanoreceptors can be classified into two groups based on the location in the body. Kinaesthetic receptors are located in muscles, tendons and joints of the body and cutaneous receptors located in the skin. Nowadays, haptics technology is developing to stimulate both of these systems.

The word Haptic, based on an ancient Greek word called haptios, means related with touch. As an area of robotics, haptics technology provides the sense of touch for robotic applications that involve interaction with human operator and the environment. The sense of touch accompanied with the visual feedback is enough to gather most of the information about a certain environment. It increases the precision of teleoperation and sensation levels of the virtual reality (VR) applications by exerting physical properties of the environment such as forces, motions, textures. Currently, haptic devices find use in many VR and teleoperation applications such as computer aided design, entertainment, education, training, rehabilitation, nano-manipulation, virtual prototyping and virtual sculpturing.

Various types of haptic devices are developed, and they are employed in different types of tasks. Especially for accurate teleoperation and precision required VR applications, high precision haptic systems are required with respect to the current commercially available haptic devices. In order to meet this precision criterion, in this work, the aim is to design and manufacture a 6-DOF high precision desktop haptic device.

This paper focuses on the integration of a general purpose 6-DoF haptic desktop interface along with its mechanical, electromechanical and electronics components. The design criteria of the system are listed as high stiffness, high precision and high loading capacity (high force-feedback capability). The design process of the device is outlined in [1]. The system is selected to have hybrid structure that is composed of a 3-DoF parallel mechanism for translational motions and a 3-DoF serial mechanism for rotational motion.

The parallel mechanism is a modified R-Cube mechanism and it is actuated with direct driven brushless DC motors to simulate point-type of contact. The mechanism for rotational motions is a passive mechanism with only position sensors to monitor the motion of the handle.

The next section provides a brief summary on the haptic devices. Haptic devices are classified by their haptic sensation types, and mechanism types. The fundamentals and basic components of a haptic device design are also described in the following section. The next section is dedicated to design, analysis and simulations of the mechanism. Also, in this section, the design criteria are listed and discussed, the design procedure is presented both for translation and orientation mechanism along with the kinematics analysis for the mechanism. The manufacturing processes of the mechanism are explained in Section 5. Finally, in the last section, the integration of the mechanical, electro-mechanical and electronic components are presented, part selection and integration of the complete system is described and experimental results are provided and discussed.

2. Background

Wide variety of types and sizes of haptic devices are utilized in various state-of-the-art applications for both scientific and commercial purposes. Haptics technology is usually used for complex tasks such as controlling a manipulator in hazardous environments, minimal invasive surgery, robotic rehabilitation, nano-manipulation task, 3D design, education, and training applications.

In this section, the aim is to describe previous haptic applications and clarify the concept of haptics. In order to achieve this objective haptics technology is investigated in three separate groups by their: (1) feedback types, and (2) mechanical structures.

2.1. Kinaesthetic and Cutaneous Haptic Devices

Kinaesthetic receptors are located in muscles, tendons and joints of the body as shown in Fig. 1(a). The kinaesthetic system refers to the awareness of force, motion, position and low frequency vibration. Cutaneous receptors are located in the dermis and epidermis layer of skin as shown in Fig. 1(b). Cutaneous system refers to the awareness of touch, pressure, stretch, texture and high frequency vibration.

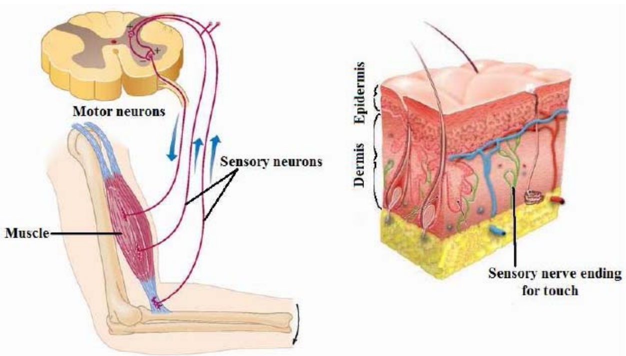

(a) (b)

Fig. 1. Types of mechanoreceptors receptors: (a) Kinaesthetic, (b) Cutaneous [2]

Kinaesthetic display devices are human–computer interfaces that can simulate kinaesthetic parameters of an environment or an object, such as motion, location, weight and rigidity. Recently, kinaesthetic haptic devices are the most common type of haptic interfaces. Several types of robot arm mechanisms have already been configured as kinaesthetic haptic devices. However, it is still an active field of research and development. Wearable haptic devices [3 & 4] and desktop haptic devices [5 & 6] are the most common device types of this class. An example of a haptic desktop device is shown in Fig. 2.

Fig. 2. Prototype of 3-DOF parallel-type haptic device [6]

Cutaneous display devices are human–computer interfaces that can copy tactile parameters of a surface such as texture, shape, roughness and temperature. Cutaneous device technology has been developed making use of several technologies such as mechanical needles actuated by electro-magnetics, piezoelectric materials, shape memory alloys and pneumatics. Various types of tactile display devices and tactile actuation systems are still an active research area. A tactile display device called VITAL1 is shown in Fig. 3. It has an 8x8 arranged pin matrix that is actuated by electro-magnetic actuators [7].

Fig. 3. VITAL1: vibrotactile display [7]

Combination of kinaesthetic and cutaneous sensation in one haptic device improves realistic hand and object interaction between user and computer. Currently most of the developed haptic interfaces are separated as, force feedback devices and tactile devices. Nevertheless some combined haptic systems that have the capability to stimulate both kinaesthetic and cutaneous receptors.

A pen-like haptic interface is shown in Fig. 4. The system is based on a tactile display and a vibrating module. It is also combined with PHANTOM™ haptic system in order to add kinaesthetic feedback capabilities to the pen-like haptic interface [8].

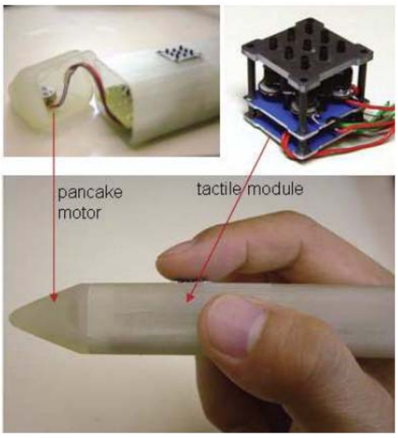

Fig. 4. Prototype of a pen-like Haptic Interface [8]

2.2. Haptic Device Mechanisms

Serial manipulators are the most common industrial robots that have been widely used variety of applications. They have serial mechanical arm structure, which is a composition of serial chain of links and joints. The main advantage of the serial manipulators is their large workspace with respect to their footprint. However their low stiffness, amplified errors from link to link due to their open kinematic structure are their main disadvantages. The serial structure has to carry and move the large weights of links and the actuators; hence it has limited loading capacities.

A parallel manipulator is a closed-loop mechanism with an end-effector placed on the moving platform that is connected to the ground with kinematic chains. Parallel manipulators have some structural advantages with respect to serial manipulators such as their higher precision, robustness and stiffness. The mechanism has to carry relatively low mass due to its ground fixed actuators. Therefore, parallel manipulators have higher loading capacity with respect to the serial manipulators. Their major disadvantage is their limited workspace, and low stiffness in singular positions.

A Hybrid manipulator is a combination of parallel and serial manipulators. They embrace the advantages of both serial and parallel manipulators.

Serial structures have been used in many haptic interface designs. Serial structure haptic devices are commercially available and probably the most well known devices are the products of Sensable Technologies [9]. The PHANTOM haptic device (Fig. 5) is currently used in various types of applications that range from commercial to scientific purposes.

Fig. 5. PHANTOM® Desktop™ Haptic Device [9]

Wearable haptic interfaces are usually designed in serial structure in order to fit the mechanism to human body. These haptic interfaces are frequently used as rehabilitation systems. An example for such an application is the wearable haptic interface shown in Fig. 6. The Maryland-Georgetown-Army (MGA) Exoskeleton has 6-DOF and it is designed and developed for shoulder rehabilitation applications [10].

Fig. 6. The MGA Exoskeleton [10]

Various researchers have recently designed several types of parallel structure haptic interfaces. Most of the published designs in the literature are based on Delta structure [6].

In Fig. 7, a modified version of Gough–Steward platform is configured as 6-DOF parallel haptic device. The system has cable-driven pantographs and rotational electrical actuators for improved workspace and output bandwidth [11].

Hybrid manipulators have the advantages of a parallel structure and serial manipulators such as high loading capacity, manipulability, stiffness, high precision, robustness and relatively large workspace. Commercial hybrid haptic devices are also available in the market for various types of applications such as Force Dimension's Delta-based haptic devices [12]. The Delta-based hybrid haptic device, Omega 6, from Force Dimension is shown in Fig. 8.

Fig. 7. 6 URS Haptic Device [11]

Fig.8. Omega 6 haptic device [12]

3. Haptic Desktop Device Components

Towards developing a new haptic desktop device, a designer has to identify the task that the haptic device will be employed. According to the task requirements, the design criteria of the haptic device have to be formed and the components should be selected. Although the components of a haptic device vary depending on the outlined types of the devices, basically all haptic systems are composed of mechanical, electro-mechanical, electronics and software parts. In this section, the commonly used components of the haptic desktop devices are investigated and discussed.

3.1. Mechanical Components

Mechanical components of a haptic device can be listed as the mechanism, material and drive system. Mechanism selection is probably the most important phase in developing a haptic device. Therefore the selection procedure is outlined in the next section. In this section, only the materials and drive systems of the haptic devices are explained and discussed.

3.1.1. Materials for the mechanism

In haptic devices the specifications of the selected material for the mechanism are directly related with the quality of the haptic perception. The weight of the mechanical components must be minimized and the device has to have low inertia and high stiffness. Hence the most important specifications for the design haptic device material are;

i) Low density

ii) High strength and rigidity

In order to minimize the gravitational effects, haptic devices are manufactured from light weight materials such as aluminum, nickel, titanium alloys and plastics. Haptic devices transmit the forces that are applied by the user. Hence, the rigidity and the strength of the mechanism are important for precision and perception of the system. As a consequence strength to weight ratio is an important factor, which has to be considered in haptic device development.

Among the other alloys, aluminum alloys is the most remarkable material in haptic devices. In general aluminum alloys have reasonable price, good machinability, high corrosion resistance and vital specifications outlined above.

Non-metallic material plastics also provide good strength to weight ratio and very low cost which are used in many haptic devices. In mass production of the haptic devices, plastic injection molding is an easy manufacturing process that is used for the manufacturing of the least important parts. Hence in general, the commercial haptic devices are composed of plastic and aluminum alloy parts and the custom haptic devices include only aluminum alloy components.

3.1.2. Drive systems

In haptics, drive systems are used for the transmission of the torques from actuators to the operator and the performance of the actuation system is more important with respect to the other robotic systems. Hence selection of the appropriate drive systems considering the type of the haptic device is important. The appropriate drive systems for a haptic device can be selected depending on the two broad classes;

i) Admittance type devices

ii) Impedance type devices

Admittance haptic devices include force sensors that sense the applied force by the operator and adjust the operator's position according to the manipulated virtual or real object. Hence the traditional transmission mechanisms such as gears can be employed in admittance type haptic devices. Nevertheless, the precision loss due to the use of transmission mechanisms is an important fact, which has to be considered in haptic device design. Therefore, high efficient and precise gearing transmission technology such as harmonic drive is currently used in haptic devices. Harmonic drives provide nearly zero backlash, light weight and high torque reduction ratios. An example for an admittance type haptic interface is VISHARD7 which can be seen in Fig. 9. VISHARD7 is a 6-DOF mobile haptic interface for large remote environments. The haptic interface is built by using brushless DC motors coupled with harmonic drive gears that provide relatively high force feedback capacity [13].

Fig. 9. Mobile haptic interface VISHARD7 [13]

In contrast to the admittance haptic devices, in an impedance haptic device, position sensors sense the position of the operator, and then the computed forces are applied to the user. Therefore, impedance type haptic devices have to be back-drivable which is possible with low inertial and low frictional drive systems. Today most of the commercially available haptic desktop devices such as Phantom, Omega and Falcon are impedance type haptic systems. They are back-drivable and have a common mechanical transmission system called Capstan drive mechanism (Fig. 10). The capstan drive mechanism consists of tendon wrapped around pulley that actuates a semi-circular link. The ratio between the pulley's and the semi-circular link's diameters provides reduction that increases the force feedback capacity of the haptic systems. Capstan drive mechanism of a 1-DOF haptic paddle can be seen in Fig. 10 [14].

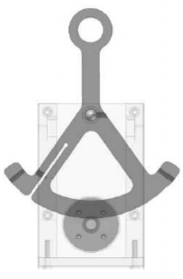

Fig. 10. Capstan drive mechanism of a haptic paddle [14]

3.2. Electro-Mechanical Components

Electro-mechanical components of a haptic desktop device can be listed as the brakes, sensors and actuators. In haptics usually two types of sensors are used; position and force/torque sensors. Position sensors measure the angles or positions of the links and this sensory input is transmitted to the computers. Depending on the type of the haptic system, force/torque sensors are also used especially in admittance type haptic devices. Moreover brakes and motors are used for the actuation of the mechanism and the properties of the actuation system are directly related with performance of the haptic device. In this section, electro-mechanical components of a haptic device is presented and discussed.

3.2.1. Brake systems

Haptic interfaces can also be categorized as active or passive interfaces depending on the employed actuators. Active haptic interfaces employ active motors, to provide active feedback to the user. On the other hand, passive haptic interfaces use dampers or brakes that dissipate the energy of the motion. In contrast to the active actuators, passive actuators such as brakes, dampers and clutches are actually stable components that they can only absorb the energy of the system. Therefore they can provide relatively larger forces without risking the user's safety. Furthermore it can improve the stability of the system. However passive actuators can only simulate some models such as high stiff wall or any rigid surface but they cannot simulate a model of an elastic surface or moving object. Nevertheless, due to the outlined advantages, dissipative components are recently employed in some haptic devices for better force-feedback capabilities and higher perception levels. Currently mechanic friction, electro-magnetic, magneto-rheological, electro-rheological brake systems are employed and tested in haptic devices.

4-DOF wearable passive haptic interface is explained in [15] that uses mechanical brake systems. The brake system of the device is located at the top of the exoskeleton and the mechanism consists of separate transmission cables for actuation with brake mechanism. In this work, the requirements of an exoskeleton haptic device such as simplicity, lightweight, high safety and hard-contact simulation are provided by passive actuation [15].

An example for hybrid actuation is the 2-DOF haptic interface that is used for medical purposes has rotational and translational axes actuated by both active and passive actuators. The combination of active motors and passive brakes improves sensation levels by reflecting the natural friction and high level force feedback of the haptic colonoscopy [16].

Electromagnetic brakes such as eddy current brakes

(ECB) are also employed in haptic systems. Some of the specifications of the ECBs such as programmable damping rates, applicability to the linear motion, high frequency responses make them very appropriate for passive haptic interfaces. The development and implementation of an ECB to a haptic interface is proposed in [17].

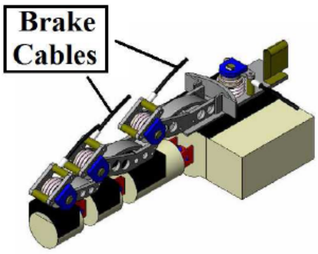

Fig. 11. Wearable passive haptic interface [15]

Magneto-rheological (MR) fluids and electro-rheological (ER) fluids are types of smart materials. They are both capable to change their viscosity reversibly within milliseconds by controlling the applied magnetic or electric field. This feature can be applied to wide range of applications such as variable damping systems. Especially in haptics due to the short response time and damping abilities of both MR and ER fluids are used as braking systems. An example of MR fluid brake system in haptic devices is presented in [18].

3.2.2. Actuators

Motors are the active actuation components in haptic devices. The performance of an active haptic device is directly related with the characteristics of the actuators. In order to provide high level sensations in a haptic interface, the actuators of the system must have low inertia, low friction, low torque ripple, high back-driveability, low backlash and high torque ratings. The selection of the appropriate actuators to meet the requirements of the haptic device is important. Currently various types of active actuators are employed in haptic desktop devices such as pneumatic, hydraulic, shape memory alloys (SMA), piezoelectric, pneumatic muscle, ultrasonic, magnetic and electrostatic actuators.

Currently, DC motors are the most common actuation systems utilized in haptic devices. Most of the haptic devices in literature, including the commercial ones are configured with DC motors. DC motors are the pioneer electrical actuation method with respect to the other actuation methods. The performance, limitations, dynamics and control methods of the DC motors are well known. Moreover, DC motors have low cost, high reliability, and simple structure. Hence in robotics, actuation with brushed or brushless DC motors is the most preferred method. However, in haptic devices other actuation systems can provide better results.

Shape memory alloys (SMA) are smart materials that have the ability to change its dimension via heat variations. Recently SMAs are employed in various types of applications including haptics. Although it seems that the SMA actuators are only employed in tactile haptic devices, SMA actuators have the potential to be used in SMA actuated haptic devices.

Pneumatics converts air pressure to rotational or linear motion. The main advantage of the pneumatic actuation is the flexibility of the actuators which is necessary in a device that interacts with human. Due to the difficulties of position and force control, the pneumatics is not common in haptic devices. An example for pneumatic parallel haptic interface is proposed by Masahiro Takaiwa et al. The proposed device is a parallel mechanism that includes 6 pneumatic actuators and potentiometers [19].

Similar to the human muscles, pneumatic muscle actuators (PMA) are contractile components work with pressurized liquid or gas. The specifications of the PMAs are similar to the conventional pneumatic actuators, but the power/weight ratios of the PMAs are relatively greater. Due to the presented advantage, PMA actuators are suitable for exoskeleton haptic devices. A 7-DOF PMA actuated exoskeleton haptic device is presented in [20].

Ultrasonic motors are piezoelectric motors that are actuated by ultrasonic vibrations. Similar to the DC motors, they consist of a rotor and a stator which is produced by piezoelectric materials. The ultrasonic motors are driven by two sinusoidal signals with a different phase. Associated with the phases of the signals the ultrasonic actuator has three phases; free, active and fixed phase. Thus, ultrasonic sensors are capable to actuate a haptic device as a hybrid (passive/active) system without using brakes or clutches. An example of such a mechanism is actuated with only four ultrasonic actuators that reflect bi-directional forces [21].

Magnetic levitation actuators are probably the most interesting ones among the other actuators. The theory is based on suspending a handle object in magnetic field. A study on developing a magnetic haptic device is presented by Berkelman et al. 6-DOF device has motion ranges of ±5 mm and ±3.5 degrees in all directions and can generate 20N force, 1.7 Nm torque [22]. A commercial magnetic levitation haptic is the product of Butterfly Haptic Inc.

3.2.2. Sensors

In haptic device design, appropriate sensor selection is important for the electro-mechanical precision of the mechanism. Essential sensors of a haptic device are force/torque and position sensors. Position sensors can be categorized in two groups; analog and digital sensors. In general, hall-effect and resistive sensors are frequently employed in haptic devices due to their high resolution and low cost.

However the noisy nature of the analog signals needs extra care during transfer and conversation to the digital signals. Besides potentiometers have various technical specifications that have to be evaluated carefully for use in haptic devices, such as mechanical resolution, linearity errors and resistance tolerance. On the other hand, digital encoders provide more accurate and noise free signal therefore digital encoders are more convenient for haptic applications. Nevertheless today, the cost of the digital encoders is relatively high and supplied resolution is limited.

Currently commercially available haptic devices are composed of both optical encoders and potentiometers. 6-DoF PHANTOM haptic device includes optical encoders and potentiometers on its active and passive joints respectively.

A variety of sensors are designed to measure forces/torques for different applications. The components of a force/torque sensor can be categorized in two groups as; the construction of the sensor and the sensing element. The construction of force sensors has to be designed considering the requirements of the application and the sensing element. Currently, strain gauges and piezoresistive sensing elements are the most common sensing elements in the force/torque sensor design. In admittance type haptic devices, both custom and commercial type force/torque sensors can be used. Although the commercial type sensors have relatively high cost, they can provide more accurate and reliable measurements.

3.3. Electronics

Data acquisition (DAQ) cards and motor amplifiers can be listed as electronic components of a haptic device. DAQ cards are the systems that measure, process, convert and transmit real world data to computers. Although the components of a DAQ system vary, depending on the specified tasks, DAQ systems may include, analog to digital converters (ADC), digital to analog converters (DAC), encoder decoders, counters, timers, digital inputs and outputs. In this section, appropriate DAQ systems for a haptic device are reviewed.

During the development of a robotic system, commercial DAQ systems provide fast and reliable environment for initial tests of the integrated mechanism. Various DAQ cards are available for haptic device development with varying low prices. The primary specification of a DAQ system in haptic device design is the sampling rate requirement of the system. The selected commercial DAQ acquisition system has to support at least 1 KHz sampling rate [23]. Moreover the supported software environments such as Simulink and LabVIEW are also important for easy programming phases and initial test of the device. Some of the commercial DAQ system providers can be listed as National Instruments (NI), Labjack, Quanser, Sensoray, Diamond Systems, dSpace, IOTech, Servo2go.

Towards developing an end product, custom designed and manufactured data acquisition cards and drives for the developed system are a necessity. As a result of the literature survey, it is observed that PIC© (Programmable Interface Controller) based DAQ cards via serial port (RS-232) is commonly used in most haptic device designs. PIC is a popular microcontroller that is developed by Microchip Technology Inc. It is used in many digital control applications due to their low cost, easy development process, wide availability and high ability.

4. Mechanism Design

This paper outlines the design of a general purpose haptic device for fine VR and teleoperation applications that require higher level of precision. In order to develop a general purpose haptic device, a kinaesthetic desktop device is selected since it supports a wide variety of applications. The hybrid mechanisms have both the advantages of serial and parallel structures as discussed in Section 2.2. Therefore, the structure of the mechanism is selected to be configured as a hybrid structure.

Table 1. Design criteria of the haptic device

Sensation	Kinaesthetic
Structure	Hybrid
Concept of Structure	Desktop Device
Footprint	<150-200 mm^2
DOF	≥6
Force feedback	Translation $\bar{u}_1$, $\bar{u}_2$, $\bar{u}_3$
Workspace	>100 W x 100 H x 100 D mm
Continuous exertable force	> 0.8 N
Nominal Resolution	< 0.1 mm

The device is designated to provide feedback signals to determine the pose of the rigid body in space, therefore it should be configured as a 6-DOF mechanism. Only point type contact is considered for this work, so the DOF can be grouped as 3-DOF active translational and 3-DOF passive rotation. Considering the task requirements the design criteria of the mechanism are listed in Table 1. The workspace, continuous exertable force and the resolution of the system are selected to be compatible with the commercial haptic desktop devices.

4.1. Conceptual Designs

According to the specified design criteria, the possible mechanism types for the hybrid structure reviewed in two groups, translation and orientation mechanisms. For translational mechanism, Delta, Cartesian Parallel, and R-Cube manipulators are considered and for orientation mechanism Agile Eye, Hybrid-Spherical and Serial-Spherical manipulators are considered in conceptual designs [1].

4.1.1. Translation mechanisms

Delta robot is a 3-DOF parallel manipulator with 3RRNR structure that is used for translational motions for various haptic device designs (Fig. 12(a)). It has seventeen links connected with twenty-one joints that are actuated by three ground fixed rotary motors. It has coupled motion and its structure provides high resolution, manipulability and high loading capacity with relatively limited workspace.

Cartesian manipulator is a 3-DOF parallel manipulator with 3PRRR structure. It can generate only translational motions (Fig. 12(b)). It has three legs that consists eleven links connected with twelve joints including base and platform. The actuation is provided by three prismatic joints with linear actuators. The motion of the manipulator is de-coupled in the direction of the prismatic axes.

R-CUBE manipulator is a 3-DOF parallel manipulator with 3NRRR structure (Fig. 12(c)). It can generate translational motions with only revolute joints. It has three legs and seventeen links connected with twenty-one revolute joints. The motion of the moving platform is directly related with the input of the first links, therefore the structure has decoupled motion making use of rotary actuators. Its kinematics analysis is simple with respect to other manipulators due to the de-coupled motion. The singularities of the manipulator only exist at the limits of the workspace which is easy to avoid [24].

4.1.2. Orientation mechanisms

Agile Eye is a 3-DOF parallel manipulator with 3RRR structure (Fig. 13(a)). Its workspace is a 140° cone with ±30° in torsion. It has eight links connected with nine joints. As a constructional advantage, it has ground fixed sensors. The structure has coupled motion.

Hybrid-Spherical is a 3-DOF hybrid manipulator with 2RE+R structure (Fig. 13(b)). Its workspace is a spherical surface with ±90°(x) ±90°(y) ±120°(z). It has four links connected with six joints. It has 2 ground fixed and 1 moving sensors.

Serial Spherical Manipulator is a 3-DOF serial manipulator with RRR structure (Fig. 13(c)). As a consequence of its serial structure, it has large workspace with a range about ±120° around all directions, but it has two moving sensors.

The comparison tables of the conceptual designs for translation and orientation mechanisms are shown in Tables 2 and 3 respectively. These two tables are used to select the configuration for the prototype of the hybrid mechanism.

Table 2. Comparison of translation mechanisms

Mechanism	Delta	Cartesian	R-CUBE
Number of Joints	21	12	24
Number of Links	17	11	17
Kinematic analysis	Complex	Simple	Simple
De-coupled motion	No	Yes	Yes
Actuation	Revolute	Prismatic	Revolute
Ground fixed motors	Yes	Yes	Yes
Types of joints	R	R-P	R

Table 3. Comparison of the orientation mechanisms

Mechanism	**Agile eye**	**Hybrid - Spherical**	**Serial-Spherical**
Number of Joints	9	6	3
Number of Links	8	4	4
Kinematic analysis	Easy	Partially Complex	Complex
De-coupled motion	No	Yes	No
Workspace	Cone 140° with ±30° torsion	±90° ±90° ±120°	±120° ±120° ±120°
Sensation	Revolute	Revolute	Revolute
Ground fixed sensors	Yes	Partially	No
Types of joints	R	R-S-Sl	R

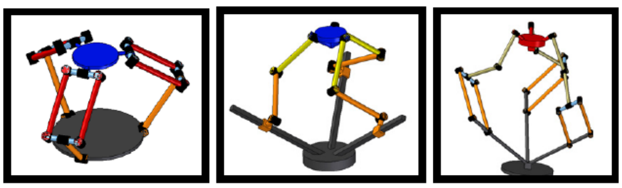

(a) (b) (c)

Fig. 12. (a) Delta, (b) Cartesian, (c) R-Cube parallel mechanism

Proceedings of the International Symposium of Mechanism and Machine Theory, 2010
AzCIFToMM – Izmir Institute of Technology
5-8 October 2010, Izmir, TURKEY

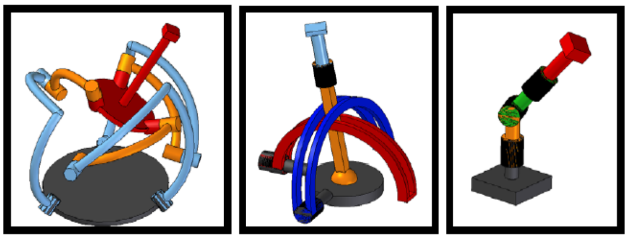

(a) (b) (c)

Fig. 13. (a) Agile Eye, (b) Hybrid-Spherical, (c) Serial-Spherical

4.2. Design of the Final Translation Mechanism

Design of the translational mechanism is presented into three sections (1) Structural design parameters, (2) Mechanical part designs and (3) Link parameter determination. In the first subsection, the design criteria of the mechanism are identified. The necessary mechanical component designs are developed in the second subsection and finally, in the third subsection the dimensions of the links are determined.

4.2.1. Structural design criteria

In the prototype mechanism, the original structure of R-CUBE had some actuation problems due to the unequally distributed gravitational effects. Hence, the original structure of R-CUBE is reoriented and the effect of gravity is distributed equally to all actuators. Apart from that, such an oriented configuration also facilitates the controller design and gravity cancellation algorithms.

The original structure configuration and the proposed configuration are shown respectively in Fig. 14(a) and 14(b). The rotation of the structure is based on isometric projection problem, which is explained in the following section [25].

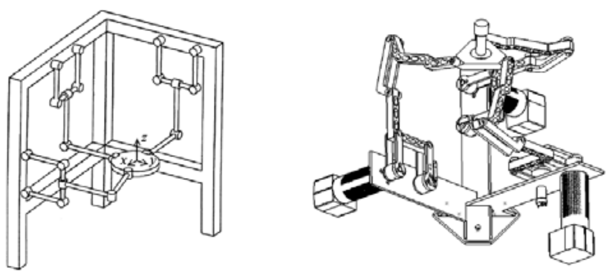

(a) (b)

Fig. 14. R-CUBE designs: (a) Original design [24], (b) Rotated design

In haptics, due to the random motion of the operator, motion through singular positions must be restricted. During the design procedure two singularity conditions are encountered which are important to avoid mechanically. One of them is already discussed in the work in [24] and presented as avoidable with a proper design. The reported singularity is at at θ_i = ±90 of the first link of the mechanism which is shown in Fig. 15(a). Although the four-bar mechanisms are reported as possible engineering trouble in [24], the problem is resolved by precise manufacturing technologies and the redundant constraint structures are used in order to avoid the singularity position mechanically (Fig. 15(b)).

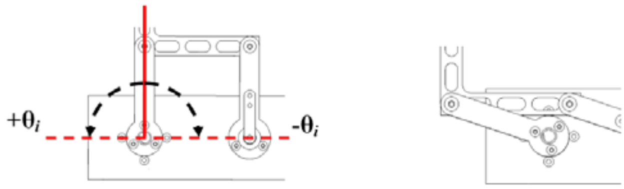

(a) (b)

Fig. 15. Singularity in the first link: (a) Singularity if θi=±90, (b) Singularity avoidance

In Fig. 16, the link lengths of the j^{th} link is denoted by l_{ij} for j=1, 2, 3, 4. The singularity at $\theta_{i4}=0$ may cause trouble at the boundaries of the workspace. Hence the link lengths of the link, l_{ij} for j=2, 3, 4 are configured to avoid any link collisions and possible singularity positions. The link length determination process is based on the iterative simulations of the mechanism that were carried out in CosmosMotion©.

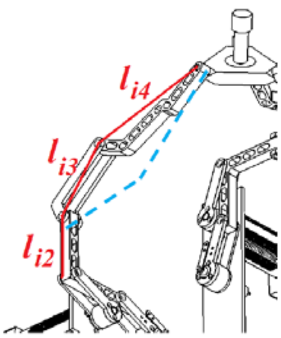

Fig. 16. Length of the second, third and fourth links

The location of the workspace is important for the compactness of the design and it is limited with the footprint of the haptic device which is specified in the design criteria table (Table 1). The graphical representations of the workspace and S_i parameter which defines the distance of the actuation axis from the origin of the base frame are shown in Fig. 17. The location of the workspace is determined with S_i parameter by identification of the dimensional limitations of the mechanism.

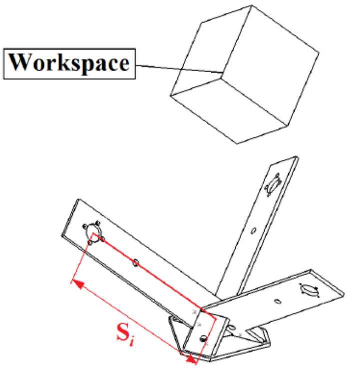

Fig. 17. The workspace and the S_i parameter of the mechanism

Lengths of the first links (Fig. 18) determine the volume of the workspace. According to the design criteria the first link length of the mechanism is calculated by direct kinematics analysis formula which is shown in detail in the following section on mechanism analysis in order to meet the 120x120x120mm workspace specification.

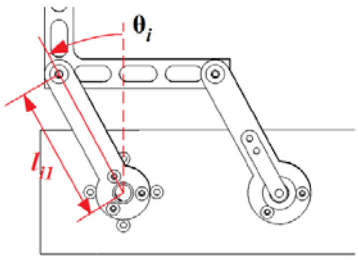

Fig. 18. Joint variables and length of the first links

4.2.2. Component design criteria

The main criterion of the parallel mechanism is to develop a universal design that is appropriate for different types of orientation mechanisms, so the moving platform of the mechanism (Fig. 19) is designed complying with this criterion. An example of this is presented in Fig. 20(a), where instead of the orientation mechanism a simple handle mechanism is mounted on the platform thus the hybrid mechanism's total DOF is decreased to 3-DOF. Similarly, mounting a 4-DOF mechanism can result in a total 7-DOF hybrid structure.

During the design of haptic desktop devices, one of the most important design specifications is the handle space that is required for operator's hand to fit ergonomically, especially when converting a standard manipulator design into a haptic device. Therefore during the design of the final mechanism, the ergonomics of the handle space is also conceived in the design phase.

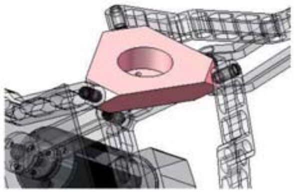

Fig. 19. Platform of the mechanism

In the design, the locations of the sensors are selected for aesthetic considerations and to have a universal design for incorporating various sensor types. The three position sensors of the mechanism mounted at the base frame on the free rocker of the four-bar mechanisms as shown in Fig. 20(a) denoted as 1, 2, 3. The position sensors of the mechanism can be replaced with various types of sensors only by remanufacturing the sensor housings. In Fig. 20(b), the sensor mechanism is shown with the sensor housing denoted as 1, the sensor as 2, the bearings as 3, and the shaft of the sensor as 4.

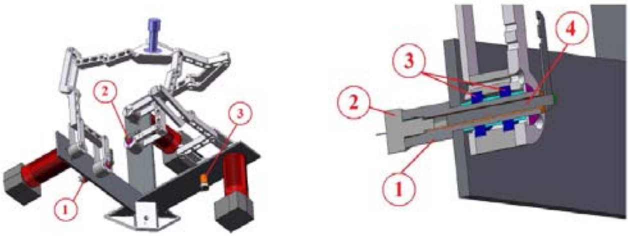

Fig. 20. Sensor locations and sensor housing designs: (a) Location of the sensors, (b) The design of the sensor housings

The CAD representation of the joint structure is shown in Fig. 21. The structure has a shaft (4), bearings (3), screws (1) and the bearing plates (2). The outer bearing plates at the left and right hand side of the image are shown in the Fig. 21. They provides leaning surface for the screws while fastening the joints. The inner bearing plate shown in the middle of the image prevents the outer races of bearings against getting stuck. The main objective in this design is to improve the mechanical precision of the joints. Besides it is also aimed to design a compact structure which has easy disassembling procedure.

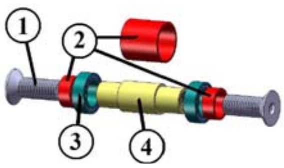

Fig. 21. CAD representation of joint components M4 screw, bearings and bearing plates

4.2.3. Link dimensioning and shape identification

Link dimensioning and shape identification of the translation mechanism are results of the structural and mechanical criteria outlined previously. The determination criteria can be listed as;

i) Dimensions of the workspace
ii) Location of the workspace
iii) Universal design
iv) Structure of the joints
v) User's handle space requirements
vi) Singularity avoidance

The lengths of the first links are determined to meet the workspace dimension specification. Previously defined 100x100x100mm workspace criterion is extended to 120x120x120mm, in order to avoid the motions in the close-range of the singular positions. The location of the workspace, which is important for the general dimensions of the mechanism, is identified with the max footprint criterion (Table 1). The universal design criterion sets the dimensions of the moving platform (Fig. 19); therefore the dimensions are determined by the size of the possible upper mechanisms. Volumes of the links are minimized to decrease the weight of mechanism. The cross-sectional area of the links is determined through the dimensions of the joint structure (Fig. 21). The second, third and the fourth link length and shape determination process is based on the iterative simulations carried out in SolidWorks© CosmosMotion© utilizing the singularity positions, link collisions and handle space ergonomics.

4.3. Design of the Final Orientation Mechanism

The serial structure proposed for the final design does not have any structural criteria. Therefore, link dimensioning and shape identification of the orientation mechanism's links is the result of criteria;

i) Sensation levels
ii) Ergonomic design
iii) Available sensors

Due to the manufacturing limitations and precision requirements, previously employed orientation mechanism of the prototype system is replaced with the serial-spherical manipulator in the final design. The orientation mechanism, serial-spherical manipulator is a 3-DOF-RRR spatial serial mechanism shown in Fig. 22.

The mechanism is designed for monitoring the rotational motions of the user's hand, so it is designed in consideration with handle ergonomics. The design is manufactured in rapid prototyping machine in our laboratories and the ergonomics of the design are evaluated.

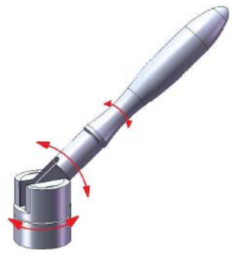

Fig. 22. Orientation mechanism

The primary challenge in the design of this mechanism is adjusting the size of the mechanism with huge amount of components, such as position sensors, bearings, cables and A/D converters. 3-DOF rotational motions of the end-effector are monitored through three miniature sensors as shown in Fig. 23(b). The A/D converters are mounted inside the mechanism (Fig. 23(a)) in order to reduce the noise level by converting the analog outputs of the position sensors to digital signals.

Fig. 23. Position sensors: (a) Location of the sensors, (b) Dimensions

The design procedure of the mechanism is finished with necessary modifications to facilitate the manufacturing process. Finally, the model is designed in CAD environment and blue-prints are prepared for the test of the ergonomics of the mechanism. The CAD design of the new configuration of the hybrid mechanism with motors, sensors, bearings is shown in Fig. 24.

Fig. 24. The CAD representation of the final design

4.4. Kinematics and Static Force Analysis

Haptic devices are the systems that are used to manipulate virtual or real systems that may be a virtual or a robotic arm. In order to control a virtual or real system by a haptic interface, the position of the handle point has to be measured then measured or calculated forces from the VR system or the slave side of the teleoperation must be reflected back to the operator. The position of the tip point, *Wr*, (Fig. 25) must be calculated with direct kinematic analysis of the parallel mechanism (R-Cube) making use of the joint sensor readings. Forces on the VR system or teleoperation slave system must be calculated or measured to restrain the operator's motion with calculated forces. In this section the position and torque calculation formulas of the developed haptic device are presented and discussed.

In Fig. 25, position of the tip point, *Wr*, is defined as the intersection point of the last link connection surfaces on the moving platform. The origin of the base coordinate frame, *O*, is located at the intersection point of the unit vectors of the coordinate frame that is originated from the respective actuator axes. The mechanism parameters, variables and the rotated coordinate axes as shown in Fig. 25 that are used in the direct and inverse kinematics analysis, and in the static torque calculations.

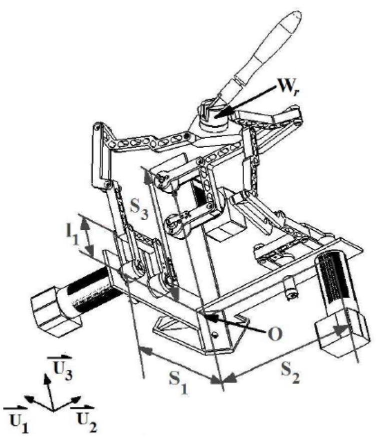

Fig. 25. Mechanism parameters

In the parallel mechanism, the translational motion of the platform is regulated by the orientation of the actuators. Due to the decoupled motion of the mechanism, the motion along $\vec{u}_1$, $\vec{u}_2$, and $\vec{u}_3$ axes is only dependent on the motors placed on the same axes which have rotations about $\vec{u}_2$, $\vec{u}_3$, and $\vec{u}_1$ axes, respectively. Therefore, the mechanism's direct and inverse kinematics analysis is relatively trivial. Nevertheless, the mechanism is only decoupled in rotated coordinate frame as shown in Fig. 25, hence the torque and position analysis of the system is carried out in rotated coordinate frame. For VR or teleoperation applications coordinate frame is reoriented with rotation sequence presented in Eq. (1), (2) and (3). The reorientation angles, α and β, are calculated by using the isometric projection representation (Fig. 26) [25].

$$\hat{C}^{(R,W)} = e^{\tilde{u}_1 \alpha} e^{\tilde{u}_2 \beta} \tag{1}$$

$$\alpha = \arcsin(\tan 30°) \cong 35.26° \tag{2}$$

$$\beta = -45° \tag{3}$$

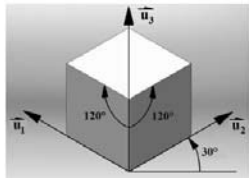

Fig. 26. Isometric projection

The control scheme of the slave system is based on the calculation of the *Wr* point by utilizing the measurements from the positions sensors. This procedure is generally called direct kinematics. In Eq. 4, the calculation of the position vector of the tip point, *Wr*, with respect to the origin point, *O*, in the ground reference frame which is presented in Fig. 25, is described.

$$\vec{Wr} = \sum_{i=1}^{3} Wr_i \vec{u}_i \tag{4}$$

Components of the *Wr* vector are a function of the rotation amounts of the actuators, θ, as shown in Eq. 5. The zero position of the angle, θ_i, is represented with dotted line in Fig. 27. In Eq. 5, S_i is the distance between motor axes and origin point and l_i is the link length of the first link which is previously presented in Fig. 25.

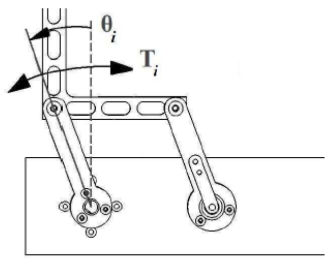

Fig. 27. Joint variable (θ_i) and torque (T_i) directions

$$Wr_i = S_i + l_i \sin(\theta_i); \qquad i = 1,2,3 \tag{5}$$

The inverse kinematics solution is given in Eq. 6, 7 and 8. In inverse kinematics solution, the mechanical structure of the four-bar mechanism limits the motion of the first link to about ±65°. Therefore, it is not possible to pass to the region where the cosines of the joint variables become negative. As a result of this, the sign ambiguity denoted with σ in Eq. 7 can be neglected and σ can be taken as +1 without the loss of generality.

$$\sin(\theta_i) = \frac{Wr_i - S_i}{l_i} \qquad i = 1,2,3 \tag{6}$$

$$\cos(\theta_i) = \sigma\sqrt{1-\sin^2(\theta_i)}; \qquad \sigma = \pm 1 \tag{7}$$

$$\theta_i = \arctan_2\left(\sin(\theta_i), \cos(\theta_i)\right) \tag{8}$$

The components of the applied force, F, are calculated in the ground reference frame in Eq. 9.

$$\vec{F} = \sum_{i=1}^{3} F_i \vec{u}_i \tag{9}$$

Torque demands for a specified force that has to be applied to the operator's hand can be formulated by Eq. 10. In Eq. 10, T is the torque required to be applied by the actuators about their respective axis of rotation as shown in Fig. 27, and F is the desired force to be applied to the operator's hand. Torque values for each actuator are calculated by taking cross product of the moment arm vector, Wr, and the force vector, F, and then taking the dot product with the respective actuator's rotation axis. The torque element in all axes that has the moment arm along its respective axis is neglected because the forces will not be transferred as a consequence of the rotation axis arrangement of links 2, 3, and 4. T is the torque applied by the actuator about each axis as shown in Fig. 25, and F is desired force to be applied to the operator's hand.

$$\begin{aligned} T_1 &= F_1(Wr_3) \\ T_2 &= F_2(Wr_1) \\ T_3 &= F_3(Wr_2) \end{aligned} \tag{10}$$

In Fig. 28, the tip point of the parallel mechanism is denoted with Wr. The orientation mechanism is in the form of a spherical wrist configuration. Thus, its forward kinematics analysis is provided as a series of pure rotations as in Eq. 11. The orientation mechanism is a passive mechanism. The inverse kinematics solution is not required since the motion of the mechanism is not controlled by any actuation system. The measured angles from this mechanism are used only for the control of the rotation motion in VR or teleoperation applications.

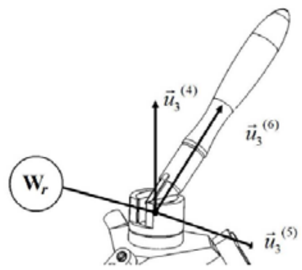

Fig. 28. *Wr* point of the mechanism

$$\hat{C}^{(3,6)} = e^{\tilde{u}_3\theta_4} e^{\tilde{u}_2\theta_5} e^{\tilde{u}_3\theta_6} \tag{11}$$

Three rotational sequences of the spherical orientation mechanism can be carried out by simple quaternion operations (Eq. 12-16) as any quaternion operator $q(\ )q^{-1}$ will rotate any vector around any axis by the desired amount of angle, provided that they are passing from a common point.

$$r_2 = q_1(r_i)q_1^{-1} \quad ; \quad q_1 = \cos\frac{\theta_4}{2} + \vec{u}_3 \sin\frac{\theta_4}{2}, \qquad q_1^{-1} = \cos\frac{\theta_4}{2} - \vec{u}_3 \sin\frac{\theta_4}{2} \tag{12}$$

$$\vec{u}_2^{(1)} = q_1(\vec{u}_2)q_1^{-1}, \quad \vec{u}_3^{(1)} = \vec{u}_3 \tag{13}$$

$$r_3 = q_2(r_2)q_2^{-1} \quad ; \quad q_2 = \cos\frac{\theta_5}{2} + \vec{u}_2^{(1)} \sin\frac{\theta_5}{2}, \qquad q_2^{-1} = \cos\frac{\theta_5}{2} - \vec{u}_2^{(1)} \sin\frac{\theta_5}{2} \tag{14}$$

$$\vec{u}_3^{(2)} = q_2\left(\vec{u}_3^{(1)}\right)q_2^{-1} \tag{15}$$

$$r_f = q_3(r_3)q_3^{-1} \quad ; \quad q_3 = \cos\frac{\theta_6}{2} + \vec{u}_3^{(2)} \sin\frac{\theta_6}{2}, \qquad q_3^{-1} = \cos\frac{\theta_6}{2} - \vec{u}_3^{(2)} \sin\frac{\theta_6}{2} \tag{16}$$

Consider that the global axes are carried to the Wr point of the mechanism, and r_i shows the initial position of the tool point. Eq. 12 represents the first rotation of r_i around $\vec{u}_3$ by angle θ_4. After calculating the new $\vec{u}_2^{(1)}$ (Eq. 13.), the second rotation θ_5 can be carried out around $\vec{u}_2^{(1)}$ to obtain r_3 (Eq. 14.). The final rotation will be performed around the precalculated $\vec{u}_3^{(2)}$ by rotation amount of θ_6 (Eq. 15, and 16). The whole rotation sequence can be represented by Eq. 17.

$$r_f = q_3 q_2 q_1 (r_i) q_1^{-1} q_2^{-1} q_3^{-1} \quad (17)$$

Although θ_4, θ_5 and θ_6 can easily be obtained from the acquired potentiometers signals, as it is required for the VR representation they should be converted into a single rotation ψ around a single rotational axis $\vec{m}$ (Eq. 18).

$$r_f = q(r_i)q^{-1} \quad ; \quad q = \cos\frac{\psi}{2} + \vec{m}\sin\frac{\psi}{2}, \quad q^{-1} = \cos\frac{\psi}{2} - \vec{m}\sin\frac{\psi}{2} \quad (18)$$

Using Eq. 17 and 18, and recalling that the quaternions have four components including one scalar and three vectoral parts, Eq. 19 and 20 can be developed to find the desired parameters ψ and m.

$$q = q_3 q_2 q_1 = a + b\vec{u}_1 + c\vec{u}_2 + d\vec{u}_3 = \cos\frac{\psi}{2} + \vec{m}\sin\frac{\psi}{2} \quad (19)$$

$$\psi = 2\cos^{-1}(a); \quad \vec{m} = \frac{b}{\sin\frac{\psi}{2}}\vec{u}_1 + \frac{c}{\sin\frac{\psi}{2}}\vec{u}_2 + \frac{d}{\sin\frac{\psi}{2}}\vec{u}_3 \quad (20)$$

It should be noted that multiplications between the quaternions should be carried out by using the rules of quaternion multiplications.

5. Manufacturing Process

The designed device is manufactured by utilizing various types of manufacturing processes, such as wire erosion, laser cutting, milling and turning for both translation and orientation mechanism. In general the manufacturing process of the entire mechanism is challenging due to;

i) Small scale parts
ii) High precision parts
iii) Parallel structure
iv) Irregular part shapes
v) Non-magnetic materials
vi) Average machinability materials

The design of the mechanism includes small bearings, bearing housings, bearing shafts, wiring and electronic component houses which are difficult to manufacture with conventional manufacturing processes. All moving parts of the mechanism are manufactured with high precision in order to detain possible backlashes and develop high precision mechanism. Non-identical and less precise parts in a parallel mechanism can also block the motion of the mechanism. As a result of the link length and shape determination process outlined in the previous section, the manufacturing of the irregular shaped parts result in a difficult and long manufacturing process. Especially, the platform of the mechanism is manufactured in several manufacturing phases. The presented materials which are discussed in the next section have average machinability and non-magnetic atomic configuration. In general magnetic materials can be clutched with magnetic clutches to the milling and turning machines, however non-magnetic materials require custom manufactured fixture in order to fix the workpiece to the machines. Manufacturing the parts of the mechanism with custom gages and fixtures increases the cost and time of the manufacturing process.

In material selection for translational mechanism, the primary objectives are to manufacture the mechanism with a material that is light, non-corrosive, and rigid. Therefore, non-ferrous metal alloys based on aluminum, zinc, nickel, copper, titanium, tungsten and cobalt are investigated and among the other non-ferrous alloys aluminum alloy 7075 is used to manufacture of the parallel mechanism. 7075 aluminum alloy includes 5.1-6.1% zinc, 2.1-2.9% magnesium, 1.2-2.0% copper, maximum 0.4% iron, less than 0.4% silicon and other metals. Its density is 0.0028 g/mm³ and it has wide application in highly stressed structural parts that range from various commercial aircraft components, aerospace to defense equipments. The material combines high strength with moderate toughness and corrosion resistance. Alloy 7075 offers reasonable price and good machinability when machined with carbide machining tools.

(a) (b)

Fig. 29. Assembled (a) translation mechanism, (b) orientation mechanism

The primary objective during the material selection of the orientation mechanism is to use ultra light materials, in order to reduce the payload amount of the platform of the mechanism. An engineering plastic, cast polyamide commonly known as Kestamid© can provide low densities with reasonable rigidity and price. Delrin material has density of 0.0014 g/mm³ and it has wide application for general purposes especially in chemical and food industries. It is resistant to corrosion and it has average machinability.

Both mechanisms, translation and orientation, are manufactured by using different materials and machining processes as discussed in this section. The assembled representations of both mechanisms are shown in Fig. 29.

6. System Integration

Haptic systems are composed of mechanical, electro-mechanical and electronics components. The mechanical component of the system is presented and manufacturing processes are explained in the previous sections. The electronics and electromechanical components such as actuators, sensors, data acquisition cards and motor amplifiers of the system are required to be selected and integrated to the system. In this section, the selection of the outlined components of the system is discussed and selected components are presented.

The basic components and the data flow among these components are shown in Fig. 30. This flow chart facilitates the identification of the correlation and data transfer between the system and the components. The control scheme of impedance type haptic system starts with the measurement of the positions of the mechanism's degrees of freedom from potentiometers via data acquisition card. The analog signals from the potentiometer are converted to digital signals by ADCs in the DAQ card. Through the reserved communication port of the PC, digital signals are transferred to the computer control software and the forces are calculated as a result of the interaction between the object and the environment in VR or teleoperation application. Afterwards, the resultant forces are transmitted back though the same way, back to the actuators of the mechanism. In a VR application, acquired signals from the motion sensors through the DAQ card are used to move a virtual object in VR screen.

The only difference in teleoperation integration of this haptic device would be that actual forces has to be measured on the slave side of teleoperation instead of calculating virtual forces in the VR environment. The slave system is usually at a distant site. Therefore, the signals between the master and the slave robot must have a communication system such as the Internet, cables or wireless technology in teleoperation systems.

Among the other actuation methods presented in the Chapter 2, DC motors are the most frequently used actuator types in the design of the robotic applications owing to their simple structure, low cost, high reliability and wide availability for various applications. DC motors are also used in the design of the haptic devices. In this work, due to their advantages outlined above, Brushless DC motors are employed in the system. Basically DC motors can be grouped in two categories as brushed and brushless DC motors. Brushed DC motors are composed of brushes, commutator, stator and rotor. Because of the switching mechanism, motor and the maintenance cost of the actuator is high and the structure of the motor is sensitive to dust and abrasion. In contrast brushless DC (BLDC) motors include only a permanent magnet rotor and a stator. In BLDCs, the switching is generated with electronic switching circuits, instead of any mechanical switching.

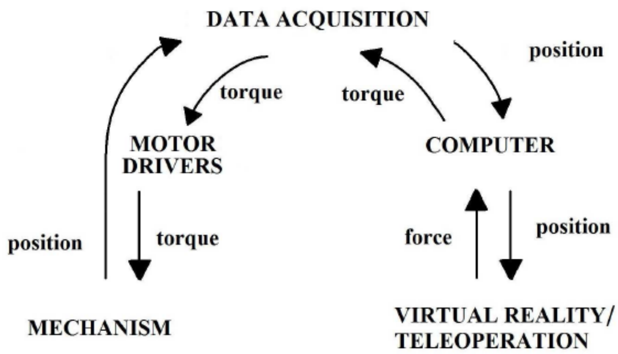

Fig. 30. Data flow

The actuators are selected as a result of the force analysis performed in the simulation studies. The applied force specification of the haptic device is to apply at least 0.8 N of force in all directions. This specification is consistent with the similar haptic devices in the market [9]. The initial selection of the actuator is a Maxon brushless DC motor that provides 310 mNm of continuous torque according to its datasheet to comply with the force requirements of the device.

In impedance type haptic devices, usually DC motors with capstan drives are used. However, it is foreseen that in time, the cables of the capstan drives loosen and results in loss of precision since the mechanism is driven without any transmission mechanism. Brushless DC (BLDC) motors are used in direct drive formation.

The system requires motor amplifiers that drive the three BLDC motors through current mode requiring +/- 10 V analogue signals as inputs. Maxon BLDC motor amplifiers (drivers) are selected to be compatible with the current requirements of the motors. These amplifiers are used to drive the actuators in current mode, which enables to drive the actuators by torque inputs that originated from the haptic controller system. The amplifiers are selected to have a response rate of at least 1 kHz.

The design of the mechanism allows using separate sensors to measure the rotation amount of each actuator. Thus, it is not required to have an encoder system at the rear end of the actuator which usually has 9-bit of resolution. The four-bar structure placed as the fist link has identical nominal lengths, which permits the same motion on each link.

A potentiometer or a higher bit resolution encoder (12-bit) can be aligned with the free link of the four-bar system and measure the same motion with more precision. In the initial system, six potentiometers that provide analogue signals, three on the parallel mechanism and three on the orientation mechanism, are used due to their low cost and simplicity. The selected potentiometer for the links of translation mechanism has linear track tapper, approximately 270o mechanical angle, ±5 resistance tolerance and 1% linearity error. In order to design a compact handle mechanism, it is required to use miniaturize potentiometers.

The potentiometers of the rotational mechanism have small dimensions about 10x11x4 mm. Although the presented components, called trimpot, are not designed for position sensing, due to the availability limitations of miniaturize size position sensors, these trimpots are used as sensors.

In order to minimize noise in the analog signal it is required to convert to digital signals directly. Therefore 16-Bit, High-Speed, ADC ADS8331 and the passive filtering components are mounted on the back of the trimpots. Finally, the integrated sensor modules are placed into the links of the mechanism. Located sensor of the second link can be seen in Fig. 31.

Fig. 31. Integration of the miniaturize position sensors

Due to the noise effects in high speed digital signals, cased ribbon cables are used for the power and data transmission between the integrated sensors and DAQ card. The array of the signal cables are composed of data, clock, positive supply, ground and enable signal cables.

A data acquisition (DAQ) card developed to convert analogue inputs from the potentiometers to digital signals to be fed into the computer and digital outputs from the computer to analogue signals to be fed into the motor amplifiers. The developed data acquisition card is a Microchip© PIC based system that has six 16-bit A/D converters and three 16-bit D/A converters. The developed data acquisition system includes three analog to digital converter, micro processor, three digital to analog converters and RS-232 communication ports.

Although various types of commercial data acquisition systems are available, due to the performance ratings, Quanser Q8 Hardware in the Loop (HIL) Board from Quanser Consulting Inc. is selected. Q8 has eight 12-bit D/A converters, eight 14-bit A/D converters whivh is enough for 6-DOF mechanism. Furthermore, it also has eight quadrature encoder inputs is for future modifications on the system's sensors. The system currently occupies three D/A converters for motor amplifiers and six A/D converters for the potentiometers of the Q8. While human motion is limited to 10 Hz, forces that are up to 1 kHz is important for the perception of the outer media. Therefore, in general, haptic devices are required to have at least 1 kHz of sampling rate in order to accurately provide the sense of touch [26]. Quanser Q8 DAO card can operate at 100 kHz sampling rates even in simultaneous acquisition.

Due to the sampling rate limitations of the developed custom data acquisition card, the initial tests of the mechanism are performed with the purchased commercial DAQ system. Nevertheless the small dimensions and wire houses transmitting the analog sensory outputs from the mechanism are impossible. Therefore, the digital signals from the embedded DAQ components are converted by developed ADC to DAC converter circuit.

Integrated mechanism can be seen in Fig. 32. The VR application, computer control scheme, DAQ components and the mechanism is denoted by 1, 2, 3, 4 in Fig. 32, respectively.

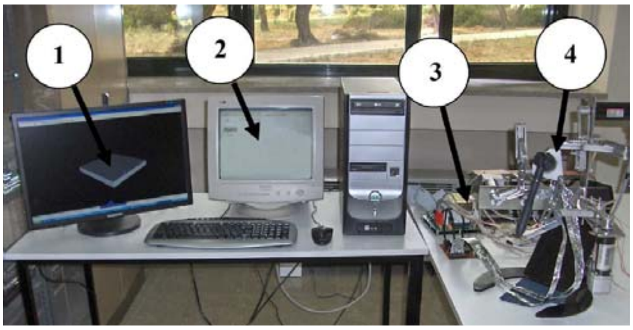

Fig. 32. The 6-DOF haptic system

7. Initial Tests and Modifications

The integrated system is tested and necessary design modifications are identified and some of them are applied system. According to the integrated system test results, necessary modifications are addressed in;

i) Rotation of the mechanism
ii) Motor selection
iii) Sensor selection

iv) Second link of the orientation mechanism

The initial test results revealed that the reoriented mechanism increased power consumption with respect to the original configuration due to the gravitational effects as shown in Table 4. Hence the orientation of the translation mechanism is changed back to the previous configuration (Fig. 33).

Table 4. Power Consumptions due to Gravitational Effects

	Motor No	Ampere
Reoriented Configuration	1	4.2
	2	4.21
	3	4.35
Original Configuration	1	0
	2	4.81
	3	0.8

Fig. 33. Modified 6-DOF mechanism

Although the technical specification sheet of the selected rate presents the motor's stall torque at 310 mNm, it is measured that the actuator can apply one third of the rated stall torque. Furthermore, changing back the orientation of the mechanism decreased the force feedback capability. Nevertheless this configuration can still provides enough torque rates to the mechanism. In order to achieve the required the feedback capacity more powerful brushed dc motors are planned to be used.

A closed-loop position control is used for gravity compensation. Fig. 34 shows the variation between torque demands for actuator 1 and different positions for actuators 1 and 2 while 3 is kept at a constant position. The torque is given in the unit of current, A, and it is experimentally measured that 1 A can be converted as about 90 mNm of torque for all actuators. It is clearly observed that gravitational effects vary as the manipulator travels. Therefore, at each instant the center of mass information should be recalculated to compensate for gravity.

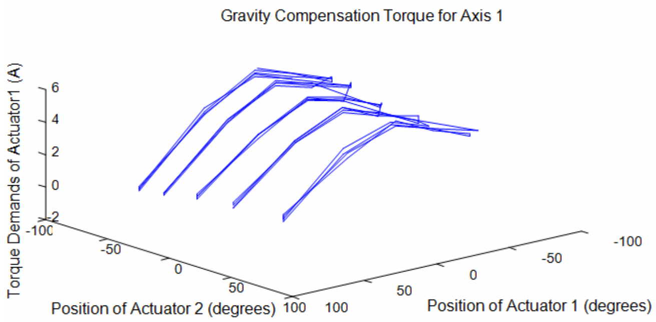

Fig. 34. Torque supplied to actuator 1 at different positions of the axes 1&2 (@ axis3: -65°)

Initially selected analog position sensors (potentiometers) provide noisy data which can results in precision loss. Therefore 12-bit three-channel incremental optical sensors can be replaced far the potentiometers.

8. Conclusions

The aim of this work is to develop a general purpose haptic device that provides higher precision ratings. Hence, previous haptic device designs are investigated, current haptic systems' sensation types are reviewed, mechanisms and their structural advantages are identified. Afterwards, the general haptic device components are listed and previously employed materials are reviewed. The difference of the admittance and impedance haptic devices is described, and drive systems are investigated according to the type of the haptic device.

Design criteria are identified and the conceptual designs are formed. Evaluating the literature survey results and the developed conceptual designs, R-CUBE mechanism is selected for reflecting three-dimensional forces and 3R serial spatial mechanism is selected for monitoring the orientation of the operator's hand. The selected mechanisms are configured as a haptic device and the dimensions and shapes of the links are determined to meet the specified design criteria. The designed mechanism is modified according to the manufacturing abilities, and then the mechanism is manufactured utilizing various manufacturing processes.

The mechanical, electro-mechanical, electronics and software parts of the device are integrated. Considering the force feedback requirements, motors are selected along with the appropriate motor amplifiers. In order to improve the precision of the actuation system, the driving type is determined as direct drive. The sensors of the system are identified and the orientation mechanism is integrated with its DAQ modules. Then, the commercial DAQ system is integrated with the other components of the mechanism. Finally initial tests are performed, necessary design changes are offered and some of them are applied to the system.

In the future the mechanism can be remanufactured with composite material in order to improve the weight/strength ratio. The electro-mechanical components such as sensors and actuators can be replaced for better accuracy and force ratings. Hence, the potentiometers can be replaced with optical encoders and the motors of the system can be changed with other types of actuators such as coreless DC motors. Furthermore, passive actuators can be integrated to the existing device; the four-bar mechanism provides unique advantage for such an implementation. The developed custom DAQ card's sampling rate can be improved with the use of more advanced technologies such as DSPs and FPGAs. VR application can be enhanced with better VR modules or custom programming. Moreover, the system can be configured as the master system of a teleoperation application.

Acknowledgments

This research was supported by a Marie Curie International Reintegration Grant within the 7th European Community Framework Programme.

References

[1]. M.I.C. Dede, O. Selvi, T. Bilgincan & Y. Kant*, Design of a haptic device for teleoperation and virtual reality systems*, IEEE International Conference on Systems, Man and Cybernetics, pages 3623 – 3628, 2009.
[2]. Web, www.medical-look.com
[3]. J. Sone, R. Inoue, K. Yamada, T. Nagae, K. Fujita & M. Sato, *Development of a Wearable Exoskeleton Haptic Interface Device*, Journal of Computing and Information Science in Engineering, vol. 8, is. 4, pages 041009-1:12, 2008.
[4]. A. Frisoli, F. Simoncini, M. Bergamasco & F. Salsedo, *Kinematic Design of a Two Contact Points Haptic Interface for the Thumb and Index Fingers of the Hand,* Journal of Mechanical Design vol. 129, is. 5, pages 520-1:10, 2007.
[5]. P. Gallina & G. Rosati, *Manipulability of a planar wire driven haptic device*, Mechanism and Machine Theory, vol. 37, is. 2, pages 215-228, 2002.
[6]. J.W. Kim, D.H. Park, H.S. Kim & S.H. Han, *Design of a Novel 3-DOF Parallel-type Haptic Device with Redundant Actuation*, International Conference on Control, Automation and Systems, Seoul, Korea, Oct. 17-20, 2007.
[7]. M. Benali-Khoudja, M. Hafez & A. Kheddar, *VITAL: An electromagnetic integrated tactile display*, Displays, vol. 28, is. 3, pages 133–144, 2007.
[8]. K.U. Kyung, J.Y. Lee & J. Park, *Design and Applications of a Pen-Like Haptic Interface with Texture and Vibrotactile Display*, Frontiers in the Convergence of Bioscience and Information Technologies, 2007.
[9]. Web, www.sensable.com
[10]. C. Carignan, J. Tang & S. Roderick, *Development of an Exoskeleton Haptic Interface for Virtual Task Training,* The 2009 IEEE/RSJ International Conference on Intelligent Robots and Systems, St. Louis, USA, October 11-15, 2009.
[11]. J.M. Sabater, R.J. Saltarén & R. Aracil, *Design, Modelling and Implementation of a 6 URS Parallel Haptic Device,* Robotics and Autonomous Systems, vol. 47, is. 1, pages 1–10, 2004.
[12]. Web, www.forcedimension.com
[13]. A. Peer & M. Buss, *A New Admittance-Type Haptic Interface for Bimanual Manipulations*, IEEE/ASME Transactions On Mechatronics vol. 13, is. 4, pages 416–428, 2008.
[14]. K. Bowen & M. K. O'Malley, *Adaptation of Haptic Interfaces for a LabVIEW-based System Dynamics Course,* Symposium on Haptic Interfaces for Virtual Environment and Teleoperator Systems, Alexandria, Virginia, USA, March 25 – 26, 2006.
[15]. M.J. Lelieveld & T. Maeno, *Design and Development of a 4 DOF Portable Haptic Interface with Multi-Point Passive Force Feedback for the Index Finger,* IEEE International Conference on Robotics and Automation, Orlando, Florida, USA, May 2006.
[16]. E., Samur, L. Flaction, U. Spaelter & H. Bleuler, A Haptic Interface with Motor/Brake System for Colonoscopy Simulation Symposium on Haptic Interfaces for Virtual Environment and Teleoperator Systems, Reno, Nevada, USA, 13-14 March, 2008.
[17]. A.H.C. Gosline & V. Hayward, *Eddy Current Brakes for Haptic Interfaces: Design, Identification, and Control,* IEEE/ASME Transactions On Mechatronics, vol. 13, is. 6, pages 669–677, 2008.
[18]. W.H. Li, B. Liu, P.B. Kosasih & X.Z. Zhang, *A 2-DOF MR Actuator Joystick for Virtual Reality Applications*, Sensors and Actuators, vol. 137, is. 2, pages 308–320, 2007.
[19]. M. Takaiwa & T. Noritsugu, *Application of Pneumatic Parallel Manipulator as Haptic Human Interface,* IEEE/ASME International Conference on Advanced Intelligent Mechatronics, Atlanta, GA, USA, September 19-23, 1999.
[20]. N. Tsagarakis, D.G.Caldwell & G.A.M. Cerda, *A 7 DOF Pneumatic Muscle Actuator (pMA) Powered Exoskeleton*, IEEE International Workshop on Robot and Human Interaction Pisa, Italy, September 1999.
[21]. B.H. Choi. & H. R. Choi, A *Semi-direct Drive Hand Exoskeleton Using Ultrasonic Motor,* IEEE International Workshop on Robot and Human Interaction Pisa, Italy, September 1999.
[22]. P.J. Berkelman, R.L. Hollis & S.E. Salcudean, *Interacting with Virtual Environments using a Magnetic Levitation Haptic Interface*, IEEE/RSJ International Conference on Intelligent Robots and Systems, Pittsburgh, PA , USA, pages 117–122, August 1995.
[23]. N.A. Tanner & G Niemeyer, *High-Frequency Acceleration Feedback in Wave Variable Telerobotics*, IEEE/ASME Transactions on Mechatronics vol. 11, is. 2, pages 119-127, 2006.
[24]. W. Li, F. Gao & J. Zhang, *R-CUBE, a decoupled parallel manipulator only with revolute joints*, Mechanism and Machine Theory, Elsevier, vol. 40, is. 4, pages 467-473, 2005.
[25]. I. Carlbomand & J. Paciorek, *Planar Geometric Projections and Viewing Transformations*, ACM Computing Surveys, vol. 10, is. 4, pages 465–502, 1978.
[26]. K. Akahane, S. Hasegawa, Y. Koike & M. Sato, A Development of High Definition Haptic Controller, First Joint Eurohaptics Conference and Symposium on Haptic Interfaces for Virtual Environment and Teleoperator Systems, pages 576-577, March 2005.